Digest Journal of Nanomaterials and Biostructures Vol. 14, No. 3, July - September 2019, p. 775 - 787

THE INFLUENCE OF HEAT TREATMENT ON THE CHARACTERISTIC OF POLY(3-HEXYLTHIOPHENE-2,5-DIYL)P3HT AND):[6,6] PHENYL- C_{71} - BUTYRIC ACID METHYL ESTER (PCBM)BLEND

I. S. NAJI, A. M. MUSLIM
Physics Dept., Science College, University of Baghdad/ Baghdad / Iraq

The influence of post thermal annealing of thin poly (3-hexylthiophene) film, and poly (3-hexylthiophene):[6,6] phenyl C_{71} butyric acid methyl ester (P3HT:$PC_{71}BM$) composite were investigated regarding their structural, morphology, optical and electrical properties. The structural properties were studied by x-ray diffraction analysis. It was found that the crystallinity of both films increased upon annealing temperature, and reduce with addition of fullerene molecules to P3HT. The surface morphology of prepared films also studied by Field Emission Scanning Electron Microscope (FESEM) and Atomic Force Microscope (AFM). The first one showed that P3HT films has a smooth and homogenous morphology with small cubic crystals and after blending with $PC_{71}BM$, the surface exhibited aggregates of needle or rod-like shapes. AFM measurements for all prepared films show that the average grain size and the surface roughness increases with the increase of annealing temperature. The optical measurements show that P3HT and its blend films exhibited strong optical absorption in the visible region. The absorption of the annealed P3HT:$PC_{71}BM$ blend films become strong and red shifted in the wavelength region ascribe to P3HT, while the absorption due to PCBM contribution does not change. Hall measurements of P3HT and the blend films showed that the mobility increases with the increase of annealing temperature while the concentration of charge carriers showed opposite manner.

(Received June 13, 2019, Accepted September 4, 2019)

Keywords: Organic semiconductor, Photovoltaic polymer, Fullerene blend

1. Introduction

Solar cells are expected to solve problems of environmental pollution and exhaustion of fossil [1]. Semiconducting organic polymers play a crucial role towards the possible realization of commercial solar energy absorbers that are low manufacturing energy and costs, light weight, flexibility, and large-scale production volumes compared to conventional photovoltaic devices based on silicon [2,3].

Among the promising polymers in this category isPoly(3-hexylthiophene-2,5-diyl) also known as P3HT. It is one of the most extensively investigated conjugated polymer suitable for OSCs due to suitable absorption spectrum and potential to be manufactured at low cost [4].

P3HT has a band gap of 2.1 eV and lowest unoccupied molecular orbital (LUMO) levels at 2.7 eV. It acts as an electron donor during the photo-excitation process. The optical absorption peak of pristine P3HT is at about 550 nm wavelength [2].

It has demonstrated promising physical properties, for example, a good stability, reasonably high hole mobility in the range of 10^{-3} cm^2 V^{-1} s^-, and a field effect mobility which can be as high as 0.1–0.2 cm^2 V^{-1} s^- in high quality samples [5].

An encouraging breakthrough in realizing higher efficiencies has been achieved by mixing electron–donor-type polymers with suitable electron acceptors (bulk heterojunction [6]. In this bulk heterojunction concept, the large interfacial area between donor and acceptor phases provides sufficient charge separation as a prerequisite for solar-cell operation. To increase the power conversion efficiency strong absorption of sunlight as well as efficient charge separation and transport within the interpenetrating networks is required. Exciton dissociation is known to occur

---

[*] Corresponding author: moonbb_moonaaaa@yahoo.com

at the interface between two materials with different excited-state energy levels presenting an abrupt change in the potential (strong electric fields at the interface) [3].

A promising electron acceptor candidate for P3HT is [6,6]phenyl-C61-butyric acid methyl ester also known as C60-PCBM or simply PCBM. PCBM is a small molecule fullerene derivative with a band gap of 2.3 eV and LUMO levels at 3.8 eV with an absorption peak in the ultraviolet region. The electron mobility of PCBM is relatively low and is reported to be between 2×10^{-3} and 2×10^{-2} $cm^2 V^{-1} s^{-1}$, and because of high hole mobility, it plays the role of electron acceptor in many organic cells. P3HT is among the Polythiophene family which is a kind of conducting polymer. It is the excitation of the π-orbit electron in P3HT that gives the photovoltaic effect in the blend [2,7].

Solar cells based on a bulk heterojunction (BHJ) of regioregularpoly(3-hexylthiophene) (P3HT) (which forms the hole-transport network) and [6,6]-phenyl-C61-butyric acid methyl ester (PCBM) (which forms the electron-transport network) have been reported among the highest performing material systems to date and have been considered as the largest in researchers' investigations and studies for improving their power conversion efficiencies [8].

Even the improvement in device efficiency has brought OPCs closer to commercial viability, the lifetime and reliability of OPCs should be substantially improved. The degradation of the active layer is clearly related to exposure to oxygen, air, and light. To achieve the stability of OPCs, either the development of improved barrier materials for packing or the development of devices with less air sensitivity (or both) is required. Air stable OPCs have reportedly been achieved by inserting a solution based metal oxide as a buffer layer between the active layer and the metal cathode [9].

The Thermal annealing process has been demonstrated to considerably increase the efficiency of P3HT based LED and solar cells by reducing the free volume and the density of defects at the interface during evaporation of the solvent [10], and by enhancing interchain interactions [11].

The electrical parameters and efficiency of OSC are affected by the lifetime and device stability. The OSC lifetime is determined by intrinsic as well as the extrinsic degradation processes. The intrinsic degradation takes place independently on degradation agents coming from outside of the OSC, such as radiation and chemical substances from the atmosphere. While the extrinsic degradation mostly includes the processes triggered by penetration of molecules from ambient atmosphere into the OSC structure and/or the UV and visible radiation. The harmfulness of the ambient atmosphere is due to the penetration of oxygen and water molecules into the bulk of the OSC. The diffused oxygen forms CTC ($P3HT+–O_2$) creating band gap states in P3HT resulting in charge mobility decrease, exciton recombination and space charge formation [4].

In this work, the change in structural, morphological, and optical properties of the P3HT and its blend with $PC_{71}BM$ with post heat treatment has been studied.

2. Experimental procedure

Poly (3-hexylthiophene) (P3HT) with a molecular weight of 34.000 gm/mol and [6,6]-phenyl-C_{61}- butyric acid methyl ester (PCBM) were purchased from American Dye Source, Inc. and used without further purification.

The solution of P3HT is made by dissolving 60mg of polymer powder in 2ml of 1,2Dichlorobenzene ($C_6H_4CI_2$) with a molecular weight of 147.00 gm/mol which is a colorless to pale yellow liquid with a pleasant odor. The blend solution was also prepared by mixing 30mg of P3HT and 30mg of PCBM (1:1) weight ratio and dissolving in 2ml of 1,2Dichlorobenzene solvent. The two solutions were sonicated for 60 min in ultrasonic bath followed by hot plate stirring at 50°C for 2 hours and 18 hours without heating to obtain homogenous solutions. Finally the both solutions were filtered by PTFE filter with a pore size of 0.45μm to remove any undissolve material and got homogenous solutions. Glass substrates were cleaned in an ultrasonic bath by using acetone and isopropanol then rinsed with deionized water and dried with nitrogen gas.

The P3HT and P3HT:PCBM blend thin films were spun on substrates by spin coating system (ACE200) with speed of 1000 rpm/S for 30 second. The thickness of pristine and blend films were measured by cross section method which was about (100, and 150 nm) respectively. The films were thermally annealed at different annealing temperatures (75,100,125, and 150^{o}C). All experimental processes were carried out in air without glove box. The microstructure of films were recorded at room temperature using x-ray diffraction system(SHIMADZU,XRD-6000)withCuKα radiation(λ=0.154 nm, current 30mA, voltage 40 kV). The morphological features for P3HT and P3HT:PCBM blend were performed by using field emission scanning electron microscopy (FE-SEM) model (Hitachi 4700 field emission microscope),and atomic force microscopy(CSPM-AA3000 contact mode spectrometer, Angstrom Advanced Inc. Company). The optical properties were measured using UV-Visible SP-8001 spectrophotometer (Meterrech). The photoluminescence spectra of the P3HT and P3HT: PCBM blend were measured by Agilent Tech. Cary Eclipse Fluorescence spectrophotometer. The electrical propertieswas carried out using Hall Effect measurement system (HMS-3000, VER 3.5).

3. Results and discussion

The structural characterization of P3HT, and P3HT:PC$_{71}$BM thin films spin coated at room temperature and annealed in vacuum for 30min at temperatures equal to 100 and 150 °C were recorded by X-ray diffraction in the range of 2θ between 0 to 60°. The XRD patterns for all prepared and annealed films as pristine and as a blend show that most parts of the structure areamorphous and display a weak reflection at (100) orientation.

Fig. 1 shows the XRD spectra of as-deposited and heat treated P3HT films at 100 and 150°C. The as-deposited sample shows a single diffraction peak with a reflection (100) before annealing at 2θ=5.51° which is associated with the interdigitation of the alkyl chains of P3HT [12], while the P3HT samples which are treated at 100 and 150°C show a diffraction peak at 5.49° and 5.43° respectively, which is associated with the lamella structure of thiophene rings in P3HT [13]. The same results are found by Jung et al. [12], and Motaung et al. [13].

The peak intensity increased with increasing the heat treatement temperature from room temperature to 150°C, and there is a shift to lower 2θ angle and reduction in fullwidth at half maximum was observed. This indicate there is an increase in the crystallites size. The d-spacing were estimated from Bragg's law and the crystallites size were calculated by the Scherrer equation and all are listed in the Table 1.

It can be concluded that, by comparing this result with data from the literature [14], the discovered peak originates from the P3HT crystallites with a-axis orientation (polymer backbone parallel and side chains perpendicular to the substrate) [15] and no diffraction peaks corresponding to the P3HT crystallites with other orientations such as polymer backbone and side chains parallel to the substrate [16].

However, when P3HT blended with PC$_{71}$BM as shown in Fig. 2. The x-ray diffraction spectra for as-deposited and annealed samples shows a low peak intensity at 5.48° which is attributed to the P3HT (100) plane [17], while the sample heat treated at 100°C the pattern shows a single diffraction peak at 5.38° which was attributed to the edge-on arrangement of the (100) planes; this was attributed to the P3HT inter-chain spacing correlated with the interdigitated alkyl chain [14]. A single diffraction peak at 5.46° was appeared for film annealed at 150°C.

The X-ray results indicate that the peak intensity of P3HT:PC$_{71}$BM blend increase when the samples are heat treated at 100 and 150°C and a reduction in FWHM was observed with an increase in crystallites size and the diffraction peak shifted to a lower 2θ at 100°C.

It can be clearly seen from the all figures and table, the peak intensity of the blend (P3HT:PC$_{71}$BM) is reduced relative to the P3HT. Which is probably due to the addition of fullerene molecules which disturbs the formation of P3HT crystallites, also due to amorphous nature of PCBM [18]. P3HT has the ability to crystallize and has a stabilizing effect on blend morphology [19]. In the blend, crystalline P3HT gets interconnected with amorphous PCBM. The crystallites size of all samples increased upon annealing at 100 and 150°C. The minimum crystallite size was 8.98, and 12.83 nm for the as-prepared P3HT, and P3HT:$PC_{71}BM$ respectively. This result of decreasing in the crystallite size of P3HT films compared to the blend films has an agreement with Van Heerden [20].

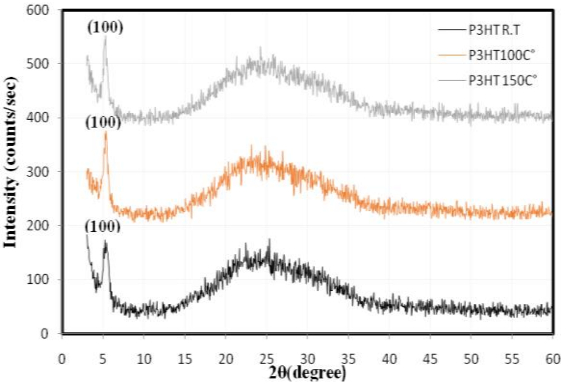

Fig. 1. The XRD pattern for as-deposited and annealed P3HT thin films.

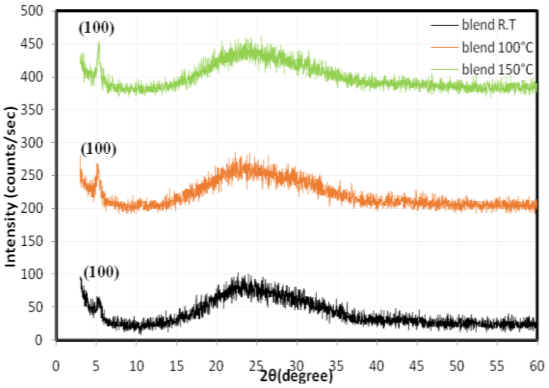

Fig. 2. The XRD pattern of as-deposited and annealed P3HT:$PC_{71}BM$ thin films.

Table 1. The structural parameters of P3HT and its blend thin films.

Sample	T_a(°C)	2θ(deg.)	d_{hkl}Exp. (nm)	d_{hkl} Theo. (nm)	hkl	FWHM (deg.)	C.S (nm)
P3HT	R.T	5.51	1.601	1.60	100	0.8857	8.98
	100	5.49	1.607	1.63	100	0.6013	13.22
	150	5.43	1.624	1.63	100	0.5596	14.21
P3HT:$PC_{71}BM$	R.T	5.48	1.61	1.63	100	0.6200	12.83
	100	5.38	1.63	1.66	100	0.6100	13.04
	150	5.46	1.61	1.63	100	0.4466	17.81

The surface morphology of the P3HT, and P3HT: $PC_{71}BM$ prepared by spin coating at room temperature and at different annealing temperature (100, 150) °C was determined by Atomic Force Microscopy (AFM) images.

Fig. 3 shows the AFM images, in two and three dimensions of as-deposited and annealed P3HT at 100 and 150°C. The morphology of the as-deposited P3HT film has a small size and a large number of grains with a roughness mean square (rms) of 0.63 nm. However, when the sample heat treated at 100 and 150°C the roughness becomes 0.324 and 1.24 nm respectively. The surface becomes rougher as the annealing temperature increased to 150°C. It is known that the higher roughness sample is better for photovoltaic application because when the surface is rough, the total surface area is much bigger than the sample with low roughness [21]. Also the grains diameter increases with increasing annealing temperature. All parameter are listed in Table 2.

However, when P3HT blended with $PC_{71}BM$ as shown in Fig. 4, the untreated sample exhibited a roughness mean square of 0.352 nm, and the roughness increase to 0.66 nm when the sample are heat treated at 150°C, also the grains diameter increase with increasing the annealing temperature.

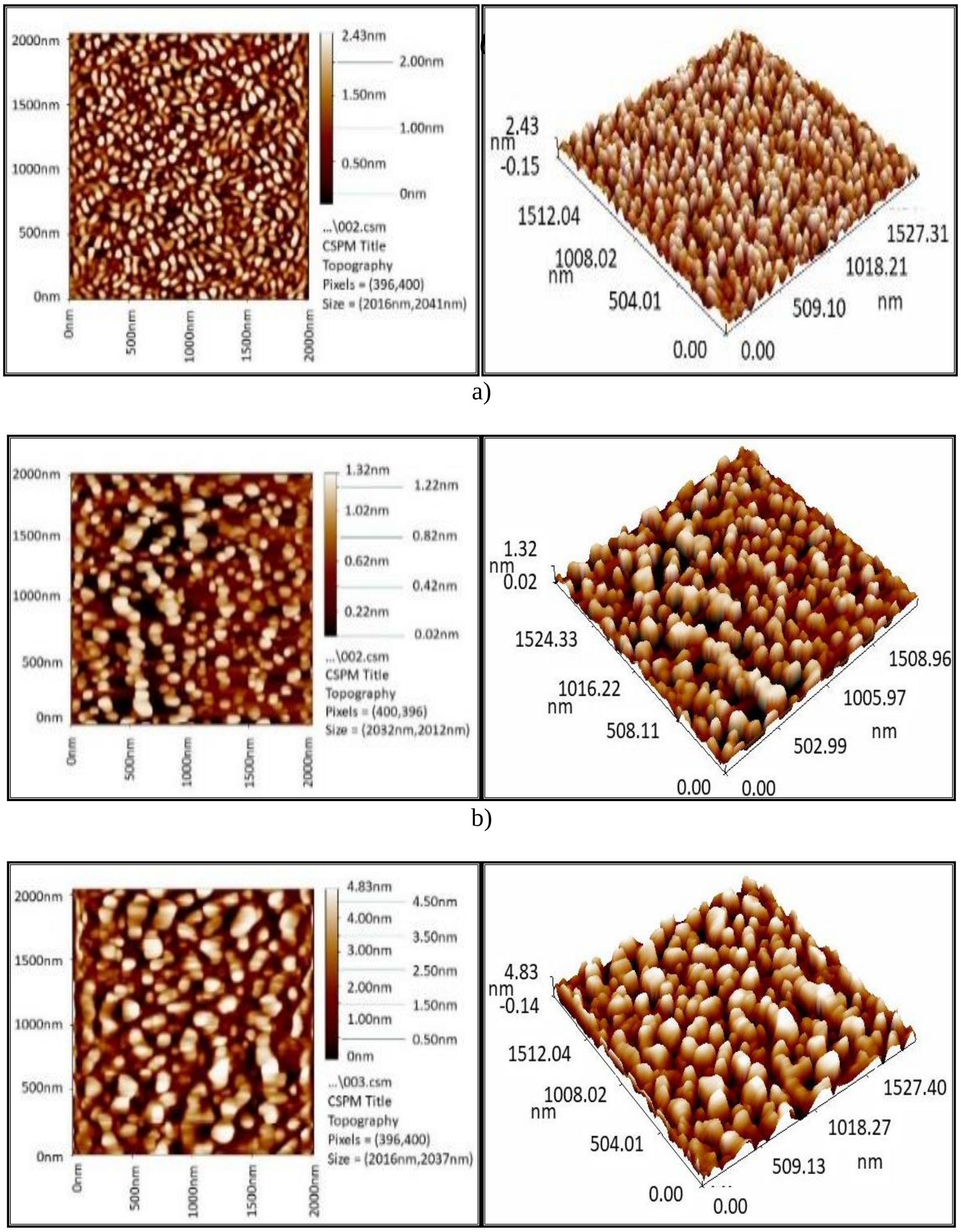

a)

b)

c)

Fig. 3. AFM images of spin coated P3HT thin films at (a) as-deposited thin film (b)Ta=100 °C (c) Ta=150 °C.

The P3HT shows high grain size than the blends which is probably due to high degree of crystallinity and self-organization beside that reason the annealing temperature increases the crystallinity of P3HT. Also the rough surface of blends is probably a signature of polymer reorganization. However, the negative result of these morphological changes is that large grain features in P3HT:PC$_{71}$BM can lead to a reduced charge collection rate at the electrodes. This is due to excessively long conduction path lengths compared to typical exciton diffusion lengths of 10 nm [22]. Since clustering of blends molecules with large grain features creates an inefficient conduction path for conjugated polymer chains to the contact electrodes, charge carrier mobilities in conjugated polymers will be diminished and result in smaller photocurrent available necessary for efficient device operation. This was noticed by Wobkenberg et al. [23], they have already shown that C$_{71}$ fullerenes combined with regioregular polymers can have comparable electron mobilities. So, small grain features with enhanced crystallinity in P3HT:PC$_{71}$BM nanocomposite films might offer better energy conversion efficiency of photoinduced carriers. This suggests that there is a thermodynamic driving force for the sample to reorganize towards a more stable equilibrium and thus to phase separate. However, excessive roughness makes phase segregation excessively comparable to the exciton diffusion length, which leads to the reduced charge segregation and device efficiencies. Similar results were also observed by Li et al. [24] and Huang-Zhong et al. [25].

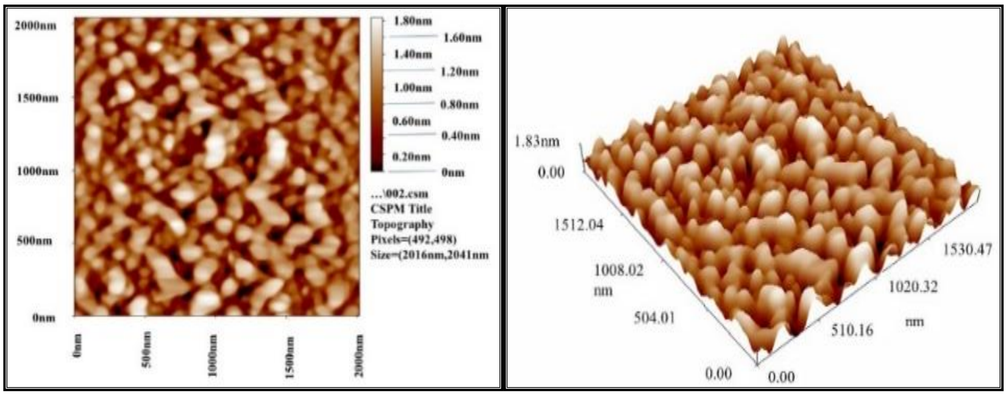

a)

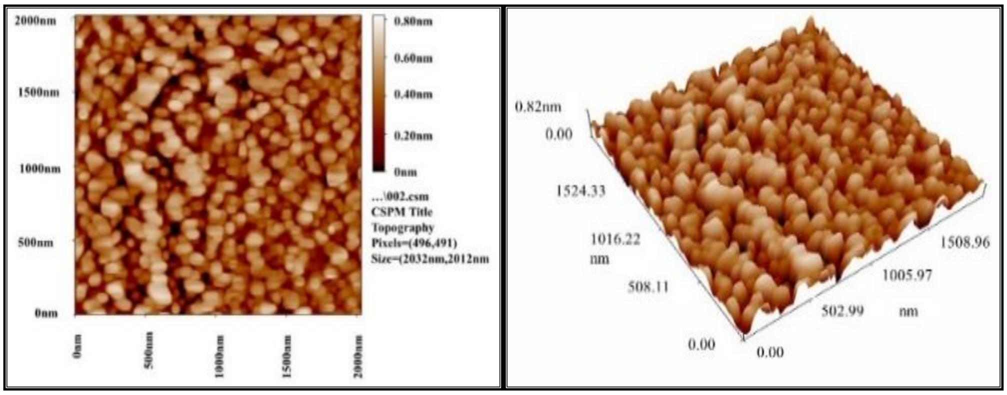

b)

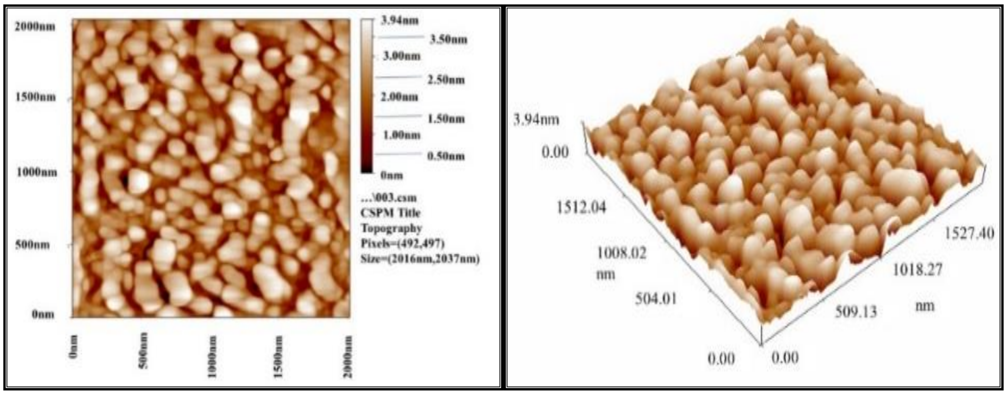

c)

Fig. 4. AFM images of P3HT:PC$_{71}$BM thin films at (a) as-deposited thin film (b)Ta=100 °C (c) Ta=150 °C.

Table 2. Grain size, Roughness average, and root mean square of as deposited and annealed films.

Sample	T$_a$ (°C)	Grain size(nm)	Roughness average (nm)	Root mean square (nm)
P3HT	R.T	68.62	0.630	0.731
	100	84.34	0.324	0.374
	150	114.25	1.240	1.430
P3HT:PC$_{71}$BM	R.T	75.36	0.352	0.419
	100	57.42	0.136	0.165
	150	92.19	0.660	0.803

Scanning electron microscopy (SEM) is a convenient method to study the surface morphology of pristine P3HT and his blends. Surface morphology of material plays an important role in solar energy conversion efficiency of the device. To achieve an efficient charge transfer and charge transport, the film morphology should be of good quality. It should be likely free from pinholes, kinks and entangling of chains.

The scanning electron microscope images of pristine P3HT film deposited on glass substrate at room temperature by spin coating with different magnification are shown in Fig. 5a. These images show a smooth and homogenous morphology with small cubic crystals. When P3HT is blended with PC$_{71}$BM the images revealed a smooth, homogenous morphology for this film as shown in Fig. 5b. It exhibited aggregates of needle or rod-like shapes. The dimensions of the rods are around 2.31µm×0.215µm.

Similar aggregates of PCBM in P3HT:PCBM film were observed by other researchers [26].

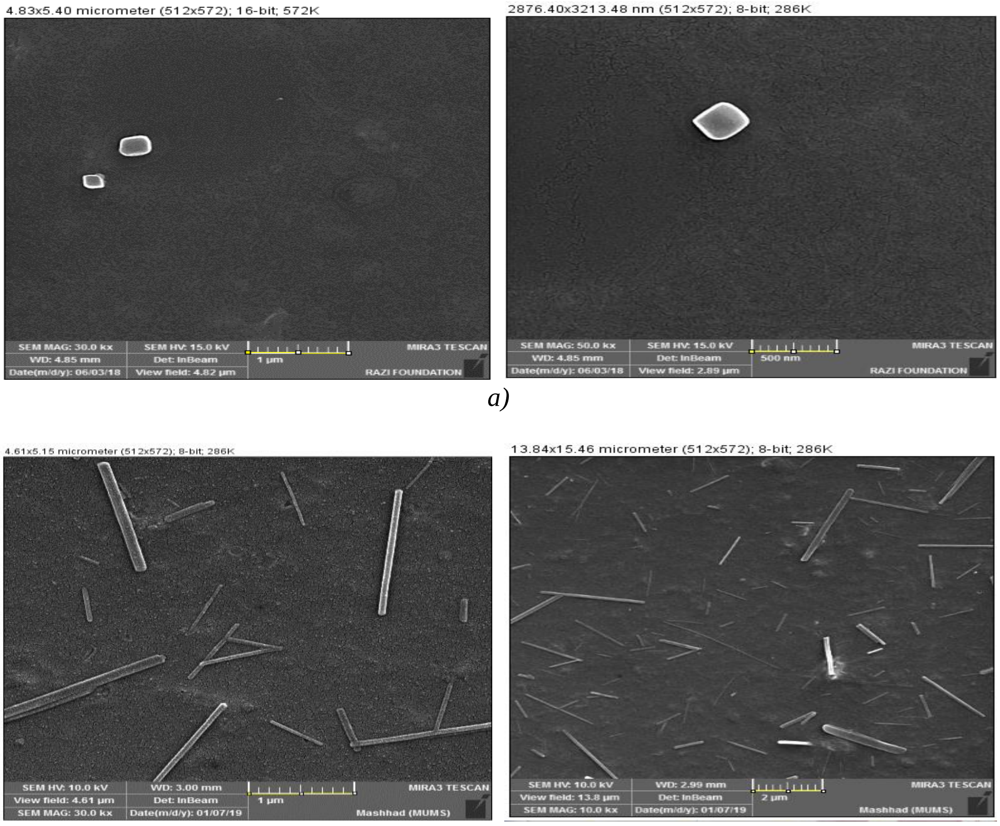

a)

b)

Fig. 5. FESEM pictures of (a)Pristine and (b)P3HT:PC$_{71}$BM film at room temperature.

To observe the growth of the PCBM crystal in P3HT: PCBM films directly and to determined the thickness of the films, cross sectional SEM was performed on the P3HT and P3HT: PCBM films deposited on glass substrate at room temperature. Fig. 6 shows the cross sectional image of the P3HT film, it is revealed the presence of 100 nm-thick pure P3HT layer and after blending the P3HT with PCBM, the SEM image showed the presence of 50 nm-thick pure PCBM layer and 100 nm-thick P3HT layer. It can be clearly seen that the PCBM crystallized from the bottom interface and obscured the original interface [27].

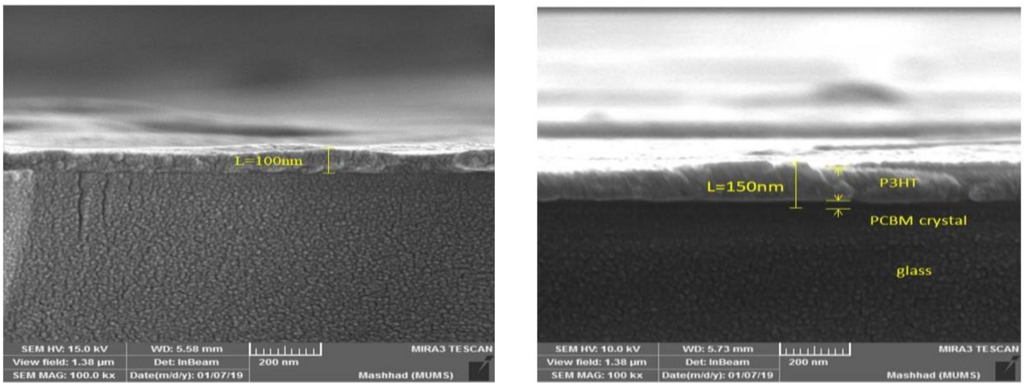

a) *b)*

Fig. 6. The cross-sectional SEM images of (a) P3HT films and (b) P3HT:PCBM films at room temperature.

Fig. 7a shows the UV-Vis absorption spectra of P3HT thin films at different annealing temperature. It can be observed that the P3HT film exhibits strong absorption in the visible wavelength range from 400-650 nm. Generally, as deposited and annealed P3HT films at different annealing temperature shows a maximum absorption around the wavelength of 555nm and a shoulder peak around the wavelength of 515nm. These bands absorption can be attributed to the π-π^* electronic transition of the P3HT conjugated backbone system [28]. While the shoulder peak around 610 nm could be related to the inter-chain stacking of P3HT molecules which suggested an enhancement in the chain ordering of the polymer [29]. It can also observed that there is no shift in the absorption peaks when the films are heat treated at different annealing temperature. But only a significant increase in the absorption intensity from 61% at room temperature to 69% after annealing the samples at 100°C. Which is indicated an increase in crystalline ordering of the polymer domain [16].

When P3HT is blended with $PC_{71}BM$ as shown in Fig. 7b, the spectra of blend films have exhibited a strong absorption spectra ranging from 320nm to 650nm which is related to the absorption of the polymer (P3HT) with maximum absorption peak at 515 nm as well as two shoulder peaks was found around 545nm and 610 nm. The presence of the shoulder peaks is due to strong inter-chain interactions which are responsible for efficient charge transportation and more optical absorption [18]. On the other hand there is a small absorption band below 400nm with a peak at 370nm which is attributed to the PCBM molecules and combined with the main peak of P3HT to form broad absorption region. When the annealing temperature increased the intensity of the absorption increase. It can be clearly seen the peak position of P3HT has a red shift from 485nm at room temperature to 515nm. This red shift indicates that the mean conjugation length of the P3HT has increased by enhancing the arrangement of the planar polymer chain as a result of thermal annealing [30]. The results are in agreement with X. Fan et al [31] and G. Li et al [24].

However, all figures show a reduction in absorption intensity of the blend compared with the P3HT before and after annealing. This reduction in intensities might be due to a tighter chain which produced by twisting of the polymer backbone or due to broken conjugation in the presence of C_{71}, thereby causing in a segments with a shorter conjugation length and weaker interchain interaction. This result can also be explained by a change in the stacking conformation of the P3HT structure from high crystallinity to lower crystallinity, and a reduction of intraplane and interplane stacking, which causes a poor π-π* transition and lower absorbance. This reduction in intensities was also observed in the literature [32,33].

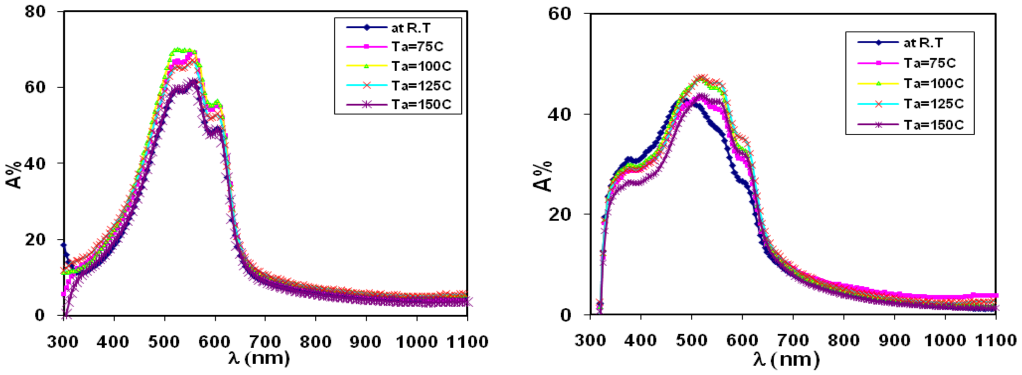

a) *b)*

Fig. 7. The absorbance spectra of P3HT:PC_{71}BM thin films at different annealing Temperatures.

The optical energy gap values (E_g^{opt}) for pristine and annealed P3HT at different annealing temperature have been determined using Tauc equation which is used to find the type of the optical transition by plotting the relations $(\alpha h\nu)^2$, $(\alpha h\nu)^{2/3}$, $(\alpha h\nu)^{1/2}$ and $(\alpha h\nu)^{1/3}$ versus photon energy (hν) and select the optimum linear part. It is found that the first relation yields linear dependence, which describes the allowed direct transition. E_g^{opt} is then determined by the extrapolation of the portion at (α=0).

Fig. 8a shows the optical energy gap of as deposited and annealed P3HT at different annealing temperature. It can be observed that there is a reduction in optical energy gap value of P3HTwhen the sample are heat treated. This results of decreasing in optical energy gap in P3HT films when applying heat to the samples has also observed by other researchers Xiaoyin et al [34]. Thus, the annealing process could be a method in reducing the optical energy gap of P3HT.

Fig. 8b shows the optical energy gap of P3HT:PC_{71}BM. It can be observed that the optical energy gap of PCBM tends to be stable around the value of 3.2eV at room temperature and when the samples heat treated at different annealing temperature. While the optical energy gap of P3HT decreases from 1.9eV at room temperature to 1.85 at 150°C. The reduction in energy gap is one of the crucial factors to obtain a good performance in the polymeric solar cells, in which that many photons can be absorbed in the active layer to generate charge carriers.

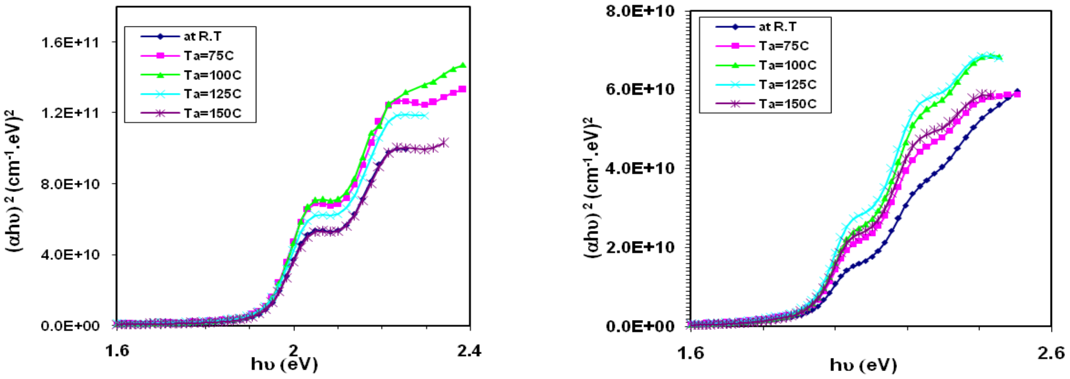

a) *b)*

Fig. 8. $(\alpha h\nu)^2$ versus photon energy (hν) of incident radiation for (a)P3HTand
(b) P3HT:PC_{71}BM thin films at different annealing temperatures.

The optical properties parameters including, energy gap, absorption coefficient, refractive index, extinction coefficient, real and imaginary part of the dielectric constant at wavelength equals to 550 nm for as deposited and annealed P3HTfilms and its blend with $PC_{71}BM$ are listed in Table 3.

Table 3. The optical constants of P3HT and its blend with $PC_{71}BM$ thin films at different annealing temperatures and λ=550 nm.

Sample	**Temp. (°C)**	**E_g^{opt}(eV)**	**α(cm^{-1}) *10^4**	**n**	**k**	**ε_r**	**ε_i**
P3HT	25	1.90	14.0	1.990	0.612	3.585	2.438
	75	1.88	15.8	1.501	0.690	1.778	2.075
	100	1.86	16.1	1.278	0.704	1.137	1.801
	125	1.87	15.3	1.673	0.670	2.350	2.242
	150	1.89	15.3	1.978	0.615	3.535	2.433
P3HT:$PC_{71}BM$	25	1.90	8.54	2.579	0.373	6.513	1.929
	75	1.86	9.74	2.544	0.414	6.305	2.108
	100	1.84	10.4	2.481	0.455	5.948	2.260
	125	1.82	10.6	2.460	0.465	5.838	2.293
	150	1.85	9.79	2.526	0.428	6.198	2.164

The photoluminescence is a powerful tool for investigating the energy levels of materials and, thereby providing fundamental information on the properties of the energy levels lying within the band gap.

Fig. 9a shows the photoluminescence emission spectra of P3HT at room temperature using an excitation wavelength of 600nm. The maximum emission peak was found to be around the wavelength of 598 nm. The PL spectra strong excitation intensity which is mostly due to the exciton-exciton annihilation [35,29].

The PL of P3HT: $PC_{71}BM$ film are shown in Fig. 9b using an exciton wavelength of 300 nm. it is observed that no peaks were found and the PL intensity of the P3HT drastically decreases in the mixture which indicates strong quenching effects in the blend compared to pure P3HT, this quenching in the P3HT: PCBM is attributed to the ultra-fast, photoinduced, donor-acceptor transfer interactions between excited polymers and the fullerene constituents in PCBM. similar results were observed by David E. Motaung et al [36] and Patrick B. et al [37].

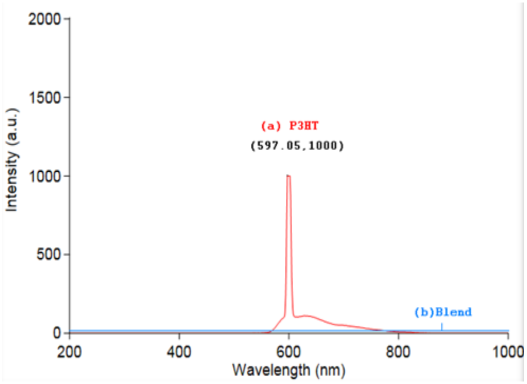

Fig. 9. Photoluminescence spectra of (a) P3HT and (b) blend solutions.

In order to determine the electrical conductivity, resistivity, type and concentration of the carrier, and carriers mobility, Hall Effect is used.

Table 4 illustrates the main parameters estimated from hall effect measurements for P3HT thin films deposited at different annealing temperature 100 and 150°C. the result showed that all films were P type. It can observe that the conductivity and the carrier mobility are increase as the annealing temperature increases .since the mobility is a function of degree of crystallinity ,crystallite size and phase domain size which are called the morphological variables, it can be concluded that the enhancement of mobility is attributed to the improvement in the crystallinity and morphology as observed in XRD, SEM and AFM analysis [38]. While the carriers concentration are decrease with heat treatment of the sample.

For P3HT blending with $PC_{61}BM$, it can be observed that there is an increase in the conductivity and the carrier mobility of the blend with the increase of annealing temperature. Such an increase, may be attributed to enhanced polymer ordering while the carriers concentration decrease.

However, when P3HT blended with $PC_{71}BM$ from Table 4 it can observe that there is an increase in the carrier mobility and the conductivity with increasing the annealing temperature wihle the carriers concentration decrease.

The blend films has higher conductivity and carrier mobility compared with the P3HT films.

It is assumed that the improved electrical properties of the blends are induced by smaller polymer and fulleren clusters formed during spin coating, which lead to the development of continuous pathways for charge carriers and an increase in the interfacial area that inhanced the exciton dissociation [39].

David E. Motaung et al [39] reported that there is an increase in the Hall mobility and coductivity of P3HT and blened films after short time annealing especially in the case of the blends. Since fullerene crystallizes out of the polymer matrix under optimized annealing conditions, leaving the polymer chains behind that will endeavour to recoganize and obtain an obtimized morphology.

Table 4. The electrical measurements of pristine P3HT and P3HT:$PC_{71}BM$ thin films at different annealing temperatures.

Sample	**Ta (°C)**	**type**	**σ x 10 $^{-5}$ $(\Omega.cm)^{-1}$**	**n *10^{11} (cm^{-3})**	**μ *10^{2} (cm/V.s)**
P3HT	R.T	P	0.3409	3.485	0.610
	100°C	P	0.4242	3.257	0.813
	150°C	p	0.6929	0.455	9.495
P3HT:$PC_{71}BM$	R.T	p	0.7365	17.88	0.025
	100°C	n	0.8055	0.247	2.034
	150°C	n	0.8680	2.478	2.187

4. Conclusion

Spin coated organic polymer (P3HT and its blend with $PC_{71}BM$) has been investigated to found the optimization annealing temperature for using in organic photovoltaic applications. There is an increase in the crystallites size with increasing annealing temperature for P3HT and its blend, while it decrease with addition of fullerene molecules which disturbs the formation of P3HT crystallites.

The surface becomes rougher as the annealing temperature increased to 150^{o}C, and Fullerene addition make the surface less rough. The annealing temperature tend to increase the P3HT optical absorption, and red shift for absorption peak. This shift is an indication of improvement the conjugation length and ordered structure of the P3HT molecules for the solar cell active layer.

References

[1] K. Yoshida, T. Oku, A. Suzuki, T. Akiyama, Y. Yamasaki, Materials Sciences and Applications **4**, 1 (2013).
[2] G. Kalonga, G. K. Chinyama, M. O. Munyati, M. Maaza, Journal of Chemical Engineering and Materials Science **4**(7), 93 (2013).
[3] Le Huong Nguyen, Harald Hoppe, Tobias Erb, SerapGünes, Gerhard Gobsch, N. Serdar Sariciftci, Adv. Funct. Mater. **17**, 1071 (2007).
[4] Jarmila Müllerová, Michal Kaiser, Vojtech Nádazdy, Peter Šiffalovic, Eva Majková, Solar Energy **134**, 294 (2016).
[5] D. Chirvase, J. Parisi, J. C. Hummelen, V. Dyakonov, Nanotechnology **15**, 1317 (2004).
[6] Christoph J. Brabec, N. Serdar Sariciftci, Jan C. Hummelen, Adv. Funct. Mater. **11**(1), (2001).
[7] H. S. Nalwa, **3**: “Conductive Polymers: Spectroscopy and Physical Properties” ISBN: 0-471-96595-2.
[8] Yasser A. M. Ismail, Tetsuo Soga, Takashi Jimbo, Int. J. New. Hor. Phys. **2**(2), 87 (2015).
[9] Kurniawan Foe, Gon Namkoong, Matthew Samson, Enas M. Younes, Ilho Nam, Tarek M. Abdel-Fattah, Hindawi Publishing Corporation, International Journal of Photoenergy **2014**, 1 (2014).
[10] P. J. Brown, D. S. Thomas, A. Ko¨hler, J. S. Wilson, J. Kim, C. M. Ramsdale, H. Sirringhaus, R. H. Friend, Physical Review B **67**(064203), 1 (2003).
[11] P. Schilinsky, C. Waldauf, C. J. Brabec, Applied Physics Letters **81**(20), 3585 (2002).
[12] J. W. Jung, W. H. Jo, In World Renewable Energy Congress-Sweden; 8-13 May; 2011; no. 057, pp. 2838-2845. Linköping University Electronic Press, 2011.
[13] D. E. Motaung, G. F. Malgas, Ch. J. Arendse, S. E. Mavundla, C. J. Oliphant, D. Knoesen, Journal of Materials Science **44**(12), 3192 (2009).
[14] U. Zhokhavets, T. Erb, H. Hoppe, G. Gobsch, N. S. Sariciftci, Thin Solid Films **496**(2), 679 (2006).
[15] T. Erb, S. Raleva, U. Zhokhavets, G. Gobsch, B. Stühn, M. Spode, O. Ambacher, Thin Solid Films **450**(1), 97 (2004).
[16] T. Erb, U. Zhokhavets, H. Hoppe, G. Gobsch, M. Al-Ibrahim, O. Ambacher, Thin Solid Films **511**, 483 (2006).
[17] L. Zhang, X. Xing, L. Zheng, Z. Chen, L. Xiao, B. Qu, Q. Gong, Scientific Reports **4**, 5071 (2014).
[18] S. Sahare, N. Veldurthi, S. Datar, T. Bhave, **5**(124), 102795 (2015).
[19] U. Zhokhavets, T. Erb, G. Gobsch, M. Al-Ibrahim, O. Ambacher, Chemical Physics Letters **418**(4-6), 347 (2006).
[20] B. A. VanHeerden, Department of Physics, University of the Western Cape, 2009.
[21] N. S. M. Shariff, P. S. M. Saad, 1 (2016).
[22] Y. Yao, C. Shi, G. Li, V. Shrotriya, Q. Pei, Y. Yang, Applied Physics Letters **89**(15), 153507 (2006).
[23] P. H. Wöbkenberg, D. D. C Bradley, D. Kronholm, J. C. Hummelen, D. M. de Leeuw, M. Cölle, T. D. Anthopoulos, Synthetic Metals **158**(11), 468 (2008).
[24] G. Li, V. Shrotriya, Y. Yao, Y. Yang, Journal of Applied Physics, **98**(4), 043704 (2005).
[25] Y. Huang-Zhong, P. J. Biao, Chinese Physics Letters **25**(4), 1411 (2008).
[26] Burak Y. Kadem, A. K. Hassan, Wayne M. Cranton, Journal of Materials Science Materials in Electronics **27**(7), 1 (2016).
[27] Y. Zhong, K. Suzuki, D. Inoue, D. Hashizume, S. Izawa, K. Hashimoto, T. Koganezawa, K. Tajima, Journal of Materials Chemistry A **4**(9), 3335 (2016).
[28] V. Shrotriya, J. Ouyang, R. J. Tseng, G. Li, Y. Yang, Chemical Physics Letters **411**(1-3), 138 (2005).
[29] B. Kadem, A. Hassan, Energy Procedia **74**, 439 (2015).
[30] M. N. Yusli, PhD diss., JabatanFizik, FakultiSains, Universiti Malaya, 2013.
[31] X. Fan, G. J. Fang, P. L. Qin, F. Cheng, X. Z. Zhao, Applied Physics A, **105**(4), 1003 (2011).
[32] D. E. Motaung, G. F. Malgas, C. J. Arendse, Synthetic Metals **160**(9-10), 876 (2010).

[33] V. D. Mihailetchi, H. X. Xie, B. de Boer, L. J. A. Koster, P. W. M. Blom, Advanced Functional Materials **16**(5), 699 (2006).

[34] X. Xiaoyin, J. Heongkyu, L. Eun-Cheol, Journal of The Korean Physical Society **57**(1), (2010).

[35] H. Wang, H. Y. Wang, B. R. Gao, L. Wang, Z. Y. Yang, X. B. Du, Q. D. Chen, J. F. Song, H. B. Sun, Nanoscale **3**(5), 2280 (2011).

[36] D. E. Motaung, G. F. Malgas, C. J. Arendse, S. E. Mavundla, D. Knoesen, **116**(1), 279 (2009).

[37] P. Boland, S. S. Sunkavalli, S. Chennuri, K. Foe, T. Abdel-Fattah, G. Namkoong, Thin Solid Films **518**, 1728 (2010).

[38] D. E. Motaung, G. F. Malgas, C. J. Arendse, T. Malwela, Materials Chemistry and Physics **124**(1), 208 (2010).

[39] D. E. Motaung, G. F. Malgas, C. J. Arendse, Journal of Materials Science **46**(14), 4942 (2011).